Heterogeneous domain adaptation: An unsupervised approach

Feng Liu, Student Member, IEEE, Guangquan Zhang, and Jie Lu, Fellow, IEEE

Abstract—Domain adaptation leverages the knowledge in one domain - the source domain - to improve learning efficiency in another domain - the target domain. Existing domain adaptation research is relatively well-progressed, but only in situations where the feature spaces of the domains are homogeneous or the target domain contains at least a few labeled instances. However, domain adaptation has not been well-studied in heterogeneous settings with an unlabeled target domain. To contribute to the research in this emerging field, this paper presents: (1) an unsupervised knowledge transfer theorem that guarantees correctness of transferring knowledge; and (2) a principal angle-based metric to measure the distance between two pairs of domains. The theorem and the metric have been implemented in an innovative transfer model, called a Grassmann-Linear monotonic maps-geodesic flow kernel (GLG), that is specifically designed for heterogeneous unsupervised domain adaptation (HeUDA). The linear monotonic maps meet the conditions of the theorem and, hence, are used to construct homogeneous representations of the heterogeneous domains. The metric shows the extent to which homogeneous representations have preserved the information in original source and target domains. Through minimizing the proposed metric, the GLG model learns homogeneous representations of heterogeneous domains and transfers knowledge through these learned representations via a geodesic flow kernel. To evaluate the model, five public datasets were reorganized into ten HeUDA tasks across three applications: cancer detection, credit assessment, and text classification. The experiments demonstrate that the proposed model delivers superior performance over the current benchmarks.

Index Terms—Transfer learning, domain adaptation, machine learning, classification.

I. Introduction

N the field of artificial intelligence (AI), and particularly in machine learning, storing the knowledge learned by solving one problem and applying it to another similar problem is very challenging. For example, the knowledge gained from recognizing cars could be used to help recognize trucks, value predictions for US real estate could help predict real estate values in Australia, or knowledge learned from classifying English documents could be used to help classify Spanish documents. As such, transfer learning models [1], [2], [3] have received tremendous attention by scholars in object recognition [4], [5], [6], [7], AI planning [8], reinforcement learning [9], [10], [11], recommender systems [12], [13], and nature language processing [14]. Compared to traditional single-domain machine learning models, transfer learning models have clear advantages. (1) The knowledge learned from in

Feng Liu, Guangquan Zhang and Jie Lu are with the Centre for Artificial Intelligence, Faulty of Engineering and Information Technology, University of Technology Sydney, Sydney, NSW, 2007, Australia, e-mail: Feng.Liu-2@student.uts.edu.au, {Guangquan.Zhang; Jie.Lu}@uts.edu.au.

one domain - the source domain - can help improve prediction accuracy in another domain - the target domain - particularly when the target domain has scant data [15]. And, 2) knowledge from a labeled domain can help predict labels for an unlabeled domain, which may avoid a costly human labeling process [16]. Of the proposed transfer learning models, domain adaptation models have demonstrated good success in various practical applications in recent years [17], [18].

Most domain adaptation models focused on homogeneous unsupervised domain adaptation (HoUDA); that is, where the source and target domains have the same, or very similar, feature spaces and there is no labeled instances in target domains. However, given the time and cost associated with human labeling, many target domains are heterogeneous and unlabeled, which means most existing HoUDA models do not perform well on the majority of target domains. Current heterogeneous unsupervised domain adaptation (HeUDA) models need parallel sets to bridging two heterogeneous domains, i.e., there are some the same or very similar instances in both heterogeneous domains. However, if the domains are confidential and private, finding similar instances between two domains is not possible, e.g., credit assessment data is confidential and private, we do not access the information of each instance. To the best of our knowledge, there are rare discussions when there is no parallel set in the HeUDA setting. This gap limits domain adaptations models to be used for more scenarios.

The aim of this research is to fill this gap by establishing a foundation for HeUDA models that predict labels for a heterogeneous and unlabeled target domain without parallel sets. This work is motivated by the observation that two heterogeneous domains may come from one domain, which means that two heterogeneous domains could be outputs of heterogeneous maps of this domain. For example, given sentences written in Latin, they can be translated into sentences written in French and Spanish. These French and Spanish sentences have different representations but share a similar meaning. If the Latin sentences are labeled by "positive", then French and Spanish sentences are probably labeled by "positive". In this example, the domain consisting of French sentences and the domain consisting of Spanish sentences come from the Latin domain. Based on this observation, we formalize the heterogeneous unsupervised domain adaptation problem and present two key factors, V and D, to reveal similarity between two heterogeneous domains:

- 1) the variation (V) between the conditional probability density functions of both domains; and
 - 2) the distance (D) between feature spaces of the two

2

domains.

Then, homogeneous representations are constructed via preserving the original similarity between two heterogeneous domains, while allowing knowledge to be transferred. In general, small V means that two domains have similar ground-truth labeling functions and small D means that two feature spaces are close. We denote V_{He} , V_{Ho} , D_{He} and D_{Ho} by values of V and D of the original heterogeneous (He) domains and the homogeneous (Ho) representations. The basic assumption of unsupervised domain adaptation models is that two domains have similar ground-truth labeling functions. Hence, the constructed homogeneous representations must make $V_{Ho} \leq V_{He}$. Similarly, $D_{Ho} \leq D_{He}$ is expected, indicating that the distance between two feature spaces of the homogeneous representations is small. This paper mainly focus on how to construct the homogeneous representations where $V_{Ho} = V_{He}$ and $D_{Ho} = D_{He}$ (the exact homogeneous representations of two heterogeneous domains). For the representations, HoUDA models can be applied to transfer knowledge across them (HoUDA models can minimize V_{Ho} and D_{Ho}).

The unsupervised knowledge transfer theorem sets out the transfer conditions necessary to prevent negative transfer (to make $V_{Ho} = V_{He}$). Linear monotonic maps (LMMs) meet the transfer conditions of the theorem and, hence, are used to construct the homogeneous representations. Rather than directly measuring the distance between two heterogeneous feature spaces, the distance between two feature subspaces of different dimensions is measured using the principal angles of a Grassmann manifold. This new distance metric reflects the extent to which the homogeneous representations have preserved the geometric relationship between the original heterogeneous domains (to make $D_{Ho} = D_{He}$). It is defined on two pairs of subspace sets; one pair of subspace sets reflects the original domains, the other reflects the homogeneous representations. Homogeneous representations of the heterogeneous domains are constructed by minimizing the distance metric based on the constraints associated with LMMs, i.e., minimize $||D_{Ho}-D_{He}||_{\ell_1}$ under the constraints $V_{Ho}=V_{He}$. Knowledge is transferred between the domains through the homogeneous representations via a geodesic flow kernel (GFK) [4]. The complete HeUDA model resulting from this research incorporates all these elements and is called the Grassmann-LMM-GFK model - GLG for short. To validate GLG's efficacy, five public datasets were reorganized into ten tasks across three applications: cancer detection, credit assessment, and text classification. The experimental results reveal that the proposed model can reliably transfer knowledge across two heterogeneous domains when the target domain is unlabeled and there is no parallel set. The main contributions of this paper are:

- 1) an effective heterogeneous unsupervised domain adaptation model, called GLG, that is able to transfer knowledge from a source domain to an unlabeled target domain in settings where both domains have heterogeneous feature spaces and are free of parallel sets;
- 2) an unsupervised knowledge transfer theorem that prevents negative transfer for HeUDA models; and
 - 3) a new principal angle based metric shows the extent

to which homogeneous representations have preserved the geometric distance between the original domains, and reveals the relationship between two heterogeneous feature spaces.

This paper is organized as follows. Section II includes a review of the representative domain adaptation models. Section III introduces the GLG model, and its optimization process is presented in Section IV. Section V describes the experiments conducted to test the models effectiveness. Section VI concludes the paper and discusses future works.

II. RELATED WORK

In this section, homogeneous unsupervised domain adaptation models and heterogeneous domain adaptation models are reviewed, which are most related to our work. Then, GLG is compared to these models.

A. Homogeneous unsupervised domain adaptation

HoUDA is the most popular research topic, with three main techniques for transferring knowledge across domains: the Grassmann manifold method [4], [16], [19], [20], the twosample test method [21], [22], [23], [24], [25], [26], and the graph matching method [18]. GFK seeks the best of all subspaces between the source and target domains, using the geodesic flow of a Grassmann manifold to find latent spaces through integration [4]. Subspace alignment (SA) [19] maps a source PCA subspace into a new subspace which is well-aligned with the target subspace. Correlation Alignment (CORAL) [27] matches the covariance matrix of the source subspace and target subspace. Transfer component analysis (TCA) [28] applies maximum mean discrepancy (MMD [29]) to measure the distance between the source and target feature spaces and optimizes this distance to make sure the two domains are closer than before. Information-theoretical learning (ITL) [30] identifies feature spaces where data in the source and the target domains are similarly distributed. ITL also learns feature spaces discriminatively so as to optimize an information-theoretic metric as a proxy to the expected misclassification errors in the target domain. Joint distribution adaptation (JDA) [31] improves TCA by jointly matching marginal distributions and conditional distributions. Scatter component analysis (SCA) [17] extends TCA and JDA, and considers the between and within class scatter. Wasserstein Distance Guided Representation Learning (WDGRL) [32] minimizes the distribution discrepancy by employing Wasserstein Distance in neural networks. Deep adaptation networks (DAN) [33] and joint adaptation networks (JAN) [34] employee MMD and deep neural networks to learn the best representations of two domains.

B. Heterogeneous domain adaptation

There are three types of heterogeneous domain adaptation models: heterogeneous supervised domain adaptation (HeSDA), heterogeneous semi-supervised domain adaptation (HeSDA), and unsupervised domain adaptation (HeUDA).

HeSDA/HeSSDA aims to transfer knowledge from a source domain to a heterogeneous target domain, where two domains have different features. There is less literature in this setting than for homogeneous situations. The main models are heterogeneous spectral mapping (HeMap) [35], manifold alignment-based models (MA) [36], asymmetric regularized cross-domain transformation (ARC-t) [37], heterogeneous feature augmentation (HFA) [38], co-regularized online transfer learning [14], semi-supervised kernel matching for domain adaptation (SSKMDA) [39], the DASH-N model [40], Discriminative correlation subspace model [41] and semi-supervised entropic Gromov-Wasserstein discrepancy [42].

Of these models, ARC-t, HFA and co-regularized online transfer learning only use labeled instances in both domains; the other models are able to use unlabeled instances to train models. HeMap works by using spectral embedding to unify different feature spaces across the target and source domains, even when the feature spaces are completely different [35]. Manifold alignment derives its mapping by dividing the mapped instances into different categories according to the original observations [36]. SSKMDA maps the target domain points to similar source domain points by matching the target kernel matrix to a submatrix of the source kernel matrix based on a Hilbert Schmidt Independence Criterion [39]. DASH-N is proposed to jointly learn a hierarchy of features combined with transformations that rectify any mismatches between the domains and has been successful in object recognition [39]. Discriminative correlation subspace model is proposed to find the optimal discriminative correlation subspace for the source and target domain. [42] presents a novel HeSSDA model by exploiting the theory of optimal transport, a powerful tool originally designed for aligning two different distributions.

Unsupervised domain adaptation models based on homogeneous feature spaces have been widely researched. However, HeUDA models are rarely studied due to two shortcomings of current domain adaptation models: the feature spaces must be homogeneous, and there must be at least some labeled instances in the target domain (or there must be a parallel set in both domains). Hybrid heterogeneous transfer learning model [43] uses the information of the parallel set of both domains to transfer knowledge across domains. Domain Specific Feature Transfer [44] is designed to address HeUDA problem when two domains have common features. Kernel canonical correlation analysis (KCCA) [45] was proposed to address HeUDA problems when there are paired instances in source and target domains, but this model is not valid when there are no paired instance in both domains.

C. Comparison to related work

Scatter component analysis (SCA) model, as an example for existing HoUDA models, incorporates a fast representation learning algorithm for unsupervised domain adaptation. However, this model can only transfer knowledge across homogeneous domains.

SSKMDA model, as an example for existing HeSSDA models, uses kernel matching method to transfer knowledge across heterogeneous domains. However, again, this model relies on labeled instances in the target domain to help correctly measure the similarity between the heterogeneous feature spaces (measure V and D, mentioned in Section I). GLG relies

on the unsupervised knowledge transfer theorem to maintain V and the principal angles of a Grassmann manifold to measure the distance (D) between two heterogeneous feature spaces. Therefore, GLG does not require any labeled instances. A metric based on principal angles reflects the extent to which the homogeneous representations have preserved the geometric distance $(\|D_{Ho} - D_{He}\|_{\ell_1})$ between the original heterogeneous domains. Knowledge is successfully transferred across heterogeneous domains by minimizing this metric under the conditions of the unsupervised knowledge transfer theorem.

Compared to existing HeUDA models, e.g., Kernel canonical correlation analysis (KCCA) model, they can transfer knowledge between two heterogeneous domains when both domains have paired instances and the target domain is unlabeled. However, the models are invalid when there no paired instances exist. GLG is designed to transfer knowledge without needing paired instances and is based on a theorem that prevents negative transfer.

These demonstrations fill some foundational gaps in the field of unsupervised domain adaptation, which will hopefully leads to further research advancements.

III. HETEROGENEOUS UNSUPERVISED DOMAIN ADAPTATION

Our HeUDA model, called GLG, is built around an unsupervised knowledge transfer theorem that avoids negative transfer through a variation factor V that measures the difference between the conditional probability density functions in both domains. The unsupervised knowledge transfer theorem guarantees linear monotonic maps (LMMs) against negative transfer once used to construct homogeneous representations of the heterogeneous domains (because $V_{Ho} = V_{He}$). A metric, which reflects the distance between the original domains and the homogeneous representations, ensures the distance factor D_{He} between the original domains is preserved ($D_{Ho} = D_{He}$). Thus, the central premise of the GLG model is to find the best LMM such that the distance between the original domains is preserved.

A. Problem statement and notation settings

Following our motivation (two heterogeneous domains may come from one domain), we first give a distribution $\mathcal P$ over a random multivariable $\mathbf x$ defined on an instance set $\mathcal X$, $\mathbf x:\mathcal X\to\mathbb R^k$ and a target function $f:\mathbb R^k\to[0,1]$. The value of $f(\mathbf x)$ corresponds to the probability that the label of $\mathbf x$ is 1. In this paper, we use $P(y=1|\mathbf x)$ to represent $f(\mathbf x)$, where y is the label of $\mathbf x$ and $y\in\{-1,1\}$. The random multivariables of feature spaces of two heterogeneous domains are heterogeneous images of $\mathbf x$:

$$\mathbf{x_s} = R_s(\mathbf{x}), \quad \mathbf{x_t} = R_t(\mathbf{x}),$$
 (1)

where $R_s: \mathbb{R}^k \to \mathbb{R}^m$, $R_t: \mathbb{R}^k \to \mathbb{R}^n$, $\mathbf{x_s} \sim \mathcal{P}_s$ and $\mathbf{x_t} \sim \mathcal{P}_t$. In the heterogeneous unsupervised domain adaptation setting, $m \neq n$ and we can observe a source domain $\mathbf{D_s} = \{(x_{si}, y_{si})\}_{i=1}^N$ and a target domain $\mathbf{D_t} = \{(x_{ti})\}_{i=1}^N$, where $x_{si} \in \mathbb{R}^m$, $x_{ti} \in \mathbb{R}^n$ are observations of the random multivariables $\mathbf{x_s}$ and $\mathbf{x_t}$, respectively, and y_{si} , taking value

4

from $\{-1,1\}$, is the label of x_{si} . $X_s = \{(x_{si})\}_{i=1}^N$ builds up a features space of $\mathbf{D_s}$ and $X_t = \{(x_{ti})\}_{i=1}^N$ builds up a features space of $\mathbf{D_t}$ and $Y_s = \{(y_{si})\}_{i=1}^N$ builds up of a label space of $\mathbf{D_s}$. In following, $\mathbf{D_s} = (X_s, Y_s)$ and $\mathbf{D_t} = (X_t)$ for short. HeUDA problem is how to use knowledge from $\mathbf{D_s}$ to label each x_{ti} in $\mathbf{D_t}$.

B. Unsupervised knowledge transfer theorem for HeUDA

This subsection first presents relations between $P(y=1|\mathbf{x})$ and $P(y=1|\mathbf{x}_s)$ (or $P(y=1|\mathbf{x}_t)$) and then gives the definition of the variation factor (V) between $P(y=1|\mathbf{x}_s)$ and $P(y=1|\mathbf{x}_t)$. Through the definition of V, we give an unsupervised knowledge transfer theorem for HeUDA. Given a measurable subset $\omega \subset \mathcal{X}$, we can obtain the probability $c(\omega) = P(y=1|\mathbf{x}(\omega))$. So, we expect that the probability $P(y=1|R_s(\mathbf{x}(\omega)))$ and $P(y=1|R_t(\mathbf{x}(\omega)))$ are around C. If C is regarded as Latin sentences mentioned in Section I, C is regarded as Panish sentences translated from the Latin sentences. If the Latin sentences translated from the Latin sentences. If the Latin sentences are labeled by "positive" C is a positive C is a positive C in C is a positive C in C is a positive C in C

$$\frac{P(y=1|\mathbf{x}_s(\omega))}{\beta_s(y=1,\mathbf{x}_s(\omega))} = \frac{P(y=1|\mathbf{x}_t(\omega))}{\beta_t(y=1,\mathbf{x}_t(\omega))} = c(\omega), \quad (2)$$

where $\beta_s(y=1,\mathbf{x}_s(\omega))$ and $\beta_t(y=1,\mathbf{x}_t(\omega))$ are two real-value functions. Since two heterogeneous domains have a similar task (i.e., labeling sentences as "positive" or "negative"), we know $\beta_s(y=1,\mathbf{x}_s(\omega))$ and $\beta_t(y=1,\mathbf{x}_t(\omega))$ should be around 1 and have following properties for any ω .

$$\beta_s(y=1, \mathbf{x}_s(\omega)) \neq \frac{1 - c(\omega)}{c(\omega)}$$
or $\beta_t(y=1, \mathbf{x}_t(\omega)) \neq \frac{1 - c(\omega)}{c(\omega)}$. (3)

The properties described in (3) guarantee that two heterogeneous domains are similar. For example, if $\beta_s(y=1,\mathbf{x}_s(\omega))=(1-c(\omega))/c(\omega)$, we will have $P(y=1|\mathbf{x}_s(\omega))=1-c(\omega)=P(y=-1|\mathbf{x}(\omega))$, indicating that positive Latin sentences are represented by negative French sentences. Based on (2), we define the variation factor $V_{He}(P(y=1|\mathbf{x}_s(\omega)),P(y=1|\mathbf{x}_t(\omega)))$ as follows.

$$V_{He}(P(y=1|\mathbf{x}_s(\omega)), P(y=1|\mathbf{x}_t(\omega)))$$

$$= |P(y=1|\mathbf{x}_s(\omega)) - P(y=1|\mathbf{x}_t(\omega))|$$

$$= c(\omega)|\beta_s(y=1,\mathbf{x}_s(\omega)) - \beta_t(y=1,\mathbf{x}_t(\omega))|.$$
(4)

Then, the definition of the heterogeneous unsupervised domain adaptation condition follows. Satisfying this condition indicates that the knowledge has been transferred in the expected way.

Definition 1 (HeUDA condition). Given $\mathbf{x_s} \sim \mathcal{P}_s$, $\mathbf{x_t} \sim \mathcal{P}_t$ and the equality (2), if there are two maps $f_s(\mathbf{x_s}) : \mathcal{R}^m \to \mathcal{R}^r$ and $f_t(\mathbf{x_t}) : \mathcal{R}^n \to \mathcal{R}^r$, then, $\forall \omega \subset \mathcal{X}$, the heterogeneous

unsupervised domain adaptation condition can be expressed by following equality.

$$\frac{P(y=1|f_s(\mathbf{x}_s(\omega)))}{\beta_s(y=1,\mathbf{x}_s(\omega))} = \frac{P(y=1|f_t(\mathbf{x}_t(\omega)))}{\beta_t(y=1,\mathbf{x}_t(\omega))} = c(\omega), \quad (5)$$

where ω a measurable set.

If this condition is satisfied, it is clear

$$P(y=1|f_s(\mathbf{x}_s(\omega)) \neq P(y=-1|f_t(\mathbf{x}_t(\omega)),$$

and

$$V_{Ho}(P(y=1|f_s(\mathbf{x}_s(\omega)), P(y=1|f_t(\mathbf{x}_t(\omega))))$$

= $c(\omega)|\beta_s(y=1,\mathbf{x}_s(\omega)) - \beta_t(y=1,\mathbf{x}_t(\omega))|,$

indicating that f_s and f_t will not cause extreme negative transfer and $V_{He} = V_{Ho}$.

Although Definition 1 provides the basic transfer condition in HeUDA scenarios, some properties of f_s and f_t still need to be explored to determine which kind of maps satisfy this condition. Monotonic maps are one such map, defined as:

Definition 2 (monotonic map). If a map $f: \mathbb{R}^m \to \mathbb{R}^r$ satisfies the following condition

$$x_i < x_j \Rightarrow f(x_i) < f(x_j),$$

where $(x_i, <)$ and $(f(x_i), <)$ are binary relations and "<" is a strict partial order over \mathbb{R}^m and $f(\mathbb{R}^m)$, then the map f is a monotonic map.

Based on Definition 2, the proposed unsupervised knowledge transfer theorem follows.

Theorem 1 (unsupervised knowledge transfer theorem). Given $\mathbf{x_s} \sim \mathcal{P}_s$, $\mathbf{x_t} \sim \mathcal{P}_t$ and the equality (2), if there are two maps $f_s(\mathbf{x_s}) : \mathcal{R}^m \to \mathcal{R}^r$ and $f_t(\mathbf{x_t}) : \mathcal{R}^n \to \mathcal{R}^r$ satisfy that 1) $f_s(\mathbf{x_s})$ and $f_t(\mathbf{x_t})$ are monotonic maps;

2) $f_s^{-1}(f_s(\mathbf{x_s})) = \mathbf{x_s}$ and $f_t^{-1}(f_t(\mathbf{x_t})) = \mathbf{x_t}$; then $f_s(\mathbf{x_s})$ and $f_t(\mathbf{x_t})$ satisfy the heterogeneous unsupervised

domain adaptation conditions.

Proof. For simplicity, we let

$$\rho(y = 1, \mathbf{x}_s, \mathbf{x}_t) = \frac{\beta_s(y = 1, \mathbf{x}_s(\omega))P(\mathbf{x}_s(\omega))}{\beta_t(y = 1, \mathbf{x}_t(\omega))P(\mathbf{x}_t(\omega))},$$

and $\rho_{y,\mathbf{x}_x,\mathbf{x}_t}$ for short. Based on the equality (2), we have

$$\frac{P_{y,\mathbf{x}_s}(y=1,\mathbf{x}_s(\omega))}{P_{\mathbf{x}_s}(\mathbf{x}_s(\omega))} = \rho_{y,\mathbf{x}_x,\mathbf{x}_t} \frac{P_{y,\mathbf{x}_t}(y=1,\mathbf{x}_t(\omega))}{P_{\mathbf{x}_t}(\mathbf{x}_t(\omega))}$$

Let $\mathbf{z}_s = f_s(\mathbf{x}_s)$ and $\mathbf{z}_t = f_t(\mathbf{x}_t)$. Since $f_t^{-1}(f_t(\mathbf{x}_t)) = \mathbf{x}_t$ and $f_s^{-1}(f_s(\mathbf{x}_s)) = \mathbf{x}_s$, we have

$$P_{y=1,\mathbf{z}_s}(y=1,\mathbf{z}_s) = P_{y=1,\mathbf{x}_s}(y=1,f_s^{-1}(\mathbf{z}_s)),$$

 $P_{y=1,\mathbf{z}_t}(y=1,\mathbf{z}_t) = P_{y=1,\mathbf{x}_t}(y=1,f_t^{-1}(\mathbf{z}_t)),$

and

$$P_{\mathbf{z}_s}(\mathbf{z}_s) = P_{\mathbf{x}_s}(f_s^{-1}(\mathbf{z}_s)), \quad P_{\mathbf{z}_t}(\mathbf{z}_t) = P_{\mathbf{x}_t}(f_t^{-1}(\mathbf{z}_t)),$$

Because $f_s(\mathbf{x}_s)$ is a monotonic map, there must be a 1-1 map between \mathbf{x}_s and \mathbf{z}_s , that is,

$$P_{y=1,\mathbf{x}_s}(y=1,f_s^{-1}(\mathbf{z}_s)) = P_{y=1,\mathbf{x}_s}(y=1,\mathbf{x}_s).$$

Hence, we arrive at following equation.

$$\frac{P_{y,\mathbf{x}_s}(y=1,f_s^{-1}(\mathbf{z}_s))}{P_{\mathbf{x}_s}(f_s^{-1}(\mathbf{z}_s))} = \rho_{y,\mathbf{x}_x,\mathbf{x}_t} \frac{P_{y,\mathbf{x}_t}(y=1,f_t^{-1}(\mathbf{z}_t))}{P_{\mathbf{x}_t}(f_t^{-1}(\mathbf{z}_t))}.$$

That is,

$$\frac{P_{y,\mathbf{z}_s}(y=1,\mathbf{z}_s)}{P_{\mathbf{z}_s}(\mathbf{z}_s)} = \rho_{y,\mathbf{x}_x,\mathbf{x}_t} \frac{P_{y,\mathbf{z}_t}(y=1,\mathbf{z}_t)}{P_{\mathbf{z}_t}(\mathbf{z}_t)}.$$

So, we have

$$\frac{P(y=1|f_s(\mathbf{x}_s(\omega)))}{\beta_s(y=1,\mathbf{x}_s(\omega))} = \frac{P(y=1|f_t(\mathbf{x}_t(\omega)))}{\beta_t(y=1,\mathbf{x}_t(\omega))} = c(\omega),$$

and this theorem is proven.

Based on Theorem 1, we demonstrate some properties of $f_s(\mathbf{x_s})$ and $f_t(\mathbf{x_t})$ and highlight the sufficient conditions for reliable unsupervised knowledge transfer. If a mapping function from heterogeneous domains to homogeneous representations satisfies the two conditions mentioned in Theorem 1, it can transfer knowledge across domains with theoretical reliability.

C. Principal angle based measurement between heterogeneous feature spaces

In this subsection, the method for measuring the distance between two subspaces is introduced. On a Grassmann manifold $G_{N,m}$ (or $G_{N,n}$), subspaces with m (or n) dimensions of \mathbb{R}^N are regarded as points in $G_{N,m}$ (or $G_{N,n}$). This means that measuring the distance between two subspaces can be calculated by the distance between those two points on the Grassmann manifold. First, the subspaces spanned by X_s and X_t are confirmed using singular value decomposition (SVD). Then, the distance between the spanned subspaces $A = span(X_s)$ and $B = span(X_t)$ can be calculated in terms of the corresponding points on the Grassmann manifold.

There are two HoUDA models that use a Grassmann manifold in this way: DAGM and GFK. The DAGM was proposed by Gopalan et al. [16]. GFK was proposed by Gong and Grauman [4]. Both have one shortcomings: the source domain and the target domain must have feature spaces of the same dimension, mainly due to the lack geodesic flow on $G_{N,m}$ and $G_{N,n}$ ($m \neq n$). In [46], Ye and Lim successfully proposed the principal angles between two different dimensional subspaces, which helps us to measure distance between two heterogeneous feature spaces consisting of X_s and X_t . Principal angles for heterogeneous subspaces are defined as follows.

Definition 3 (principal angles for heterogeneous subspaces [46]). Given two subspaces $A \in G_{N,m}$ and $B \in G_{N,n}$ ($m \neq n$), which form the matrixes $A \in \mathbb{R}^{N \times m}$ and $B \in \mathbb{R}^{N \times n}$, the i^{th} principal vectors (p_i, q_i) , i = 1, r, are defined as solutions for the optimization problem (r = min(n, m)):

Max
$$p^T q$$

s. t. $p \in A$, $p^T p_1 = \dots = p^T p_{i-1}$, $||p|| = 1$, $q \in B$, $q^T q_1 = \dots = q^T q_{i-1}$, $||q|| = 1$,

Then, the principal angles for heterogeneous subspaces are defined as

$$cos\theta_{i} = p_{i}^{T}q_{i}, i = 1, ..., r.$$

Ye and Lim [46] prove that the optimization solution for Definition 3 can be computed using SVD. Thus, we can calculate the principal angles between different dimensional subspaces, and this idea forms the distance factor D mentioned in Section I. To perfectly define distances in subspaces of different dimensions, Ye and Lim use two Schubert varieties to prove that all the defined distances in subspaces of the same dimensions are also correct when the dimensionalities differ. This means we can calculate the distances between two subspaces of different dimensions using the principal angles defined in Definition 3. Given $A = span(X_s)$ and $B = span(X_t)$, the distance vector between X_s and X_t are defined as cosine values of principal angles between A and B, which has a following expression.

$$D_{He}(X_s, X_t) = [\sigma_1(A^T B), \sigma_2(A^T B), ..., \sigma_r(A^T B)],$$

where r = min(n, m), $\sigma_i(A^TB)$ is the i^{th} singular value of A^TB computed by SVD (the i^{th} principal angles $\theta_i = cos^{-1}(\sigma_i(A^TB))$).

If we can find two maps f_s and f_t satisfying conditions of Theorem 1, we can obtain the D_{Ho} as following.

$$D_{Ho}(f_s(X_s), f_t(X_t)) = [\sigma_1(C^T D), \sigma_2(C^T D), ..., \sigma_r(C^T D)],$$

where $C = span(f_s(X_s))$ and $D = span(f_t(X_t))$. Hence, we can measure distance between D_{He} and D_{Ho} via these singular values.

D. The proposed HeUDA model

With the unsupervised knowledge transfer theorem defined, which ensures the reliability of heterogeneous unsupervised domain adaptation, and with the principal angles of Grassmann manifolds explained, we now turn to the proposed model, GLG. The optimization solution for GLG is outlined in Section IV.

A common idea for finding the homogeneous representations of heterogeneous domains is to find maps that can project feature spaces of different dimensions (heterogeneous domains) onto feature spaces with same dimensions. However, most models require at least some instances in the target domain to be labeled to maintain the relationship between the source and target domains. Thus, the key to an HeUDA model is to find a few properties that can be maintained between the original domains and the homogeneous representations. Here, these two factors are the variation factor (V_{He} and V_{Ho}) and the distance factor (D_{He} and D_{Ho}) defined in previous subsections. Theorem 1 determines the properties the maps should satisfy to make $V_{He} = V_{Ho}$ and principal angles shows the distance between two heterogeneous (or homogeneous) feature spaces $(D_{He}$ and $D_{Ho})$, but there are still two concerns: 1) which type of mapping function is suitable for Theorem 1; and 2) which properties should the map maintain between the original domains and the homogeneous representations. The first concern with the unsupervised knowledge transfer theorem is addressed by selecting LMMs as the map of choice.

Lemma 1 (linear monotonic map). Given a map $f: \mathbb{R}^m \to \mathbb{R}^r$ with form $f(x) = xU^T$, f(x) is a monotonic map if and only if U > 0 or U < 0, where $x \in \mathbb{R}^m$ and $U \in \mathbb{R}^{r \times m}$.

Proof. $\forall x_1, x_2 \in \mathbb{R}^m$, without loss of generality, we assume $x_1 < x_2$ $(x_{1i} < x_{2i}, i = 1, ..., m)$. Because $f(x) = xU^T$, we have

$$(f(x_1))_j = \sum_{i=1}^m x_{1i}u_{ji}, \quad (f(x_2))_j = \sum_{i=1}^m x_{2i}u_{ji}, j = 1, ..., r.$$

So,

$$(f(x_1))_j - (f(x_2))_j = \sum_{i=1}^m (x_{1i} - x_{2i})u_{ji}, j = 1, ..., r.$$

Because $x_{1i} - x_{2i} < 0$ and x_1 and x_2 are any vector in \mathbb{R}^m satisfying $x_1 < x_2$, $(f(x_1))_j < (f(x_2))_j$ if and only if $u_{ji} > 0$. We can simply prove the f(x) is a decreasing monotonic map if and only if $u_{ji} < 0$.

Since the defined map in Lemma 1 only uses U and according to the generalized inverse of matrix, a matrix $f(X_s)$ must satisfy $f^{-1}(f(X_s)) = X_s$. Therefore, we can prove that LMMs satisfy the conditions in Theorem 2.

Theorem 2 (LMM for HeUDA). Given $\mathbf{x_s} \sim \mathcal{P}_s$, $\mathbf{x_t} \sim \mathcal{P}_t$ and the equality (2), if there are two maps $f_s(\mathbf{x_s}) : \mathcal{R}^m \to \mathcal{R}^r$ and $f_t(\mathbf{x_t}) : \mathcal{R}^n \to \mathcal{R}^r$ are LMMs, then $f_s(\mathbf{x_s})$ and $f_t(\mathbf{x_t})$ satisfy the HeUDA condition.

Proof. Because $f_s(X_s)$ and $f_t(X_t)$ are LMMs, they satisfy the first condition of Theorem 1, we only need to prove $f^{-1}(f(\mathbf{x_s})) = \mathbf{x_s}$. According to Moore-Penrose pseudoinverse of U_s in $f(\mathbf{x_s})$, it is obvious that the second condition of Theorem 1 can be satisfied. Hence, this theorem is proved. \square

Remark 1. From this theorem and the nature of LMMs, we know this positive map can better handle datasets that have many monotonic samples because the probabilities in these monotonic samples can be preserved without any loss. The existence of these samples has the greatest probability of preventing negative transfers.

Theorem 2 addresses the first concern and provides a suitable map, such as the map in Lemma 1, to project two heterogeneous feature spaces onto the same dimensional feature space. It is worthwhile showing that an LMM is just one among many suitable maps for Theorem 1. A nonlinear map, such as $\exp(U)$, also can be used to construct the map as long as the map is monotonic. In future work, we intend to explore additional maps suitable for further HeUDA models.

This brings us to the second concern: Which properties can be maintained during the mapping process between the original domains and the homogeneous representations. As mentioned above, the principal angles play a significant role in defining the distance between two subspaces on a Grassmann manifold, and in explaining the projections between them [47]. Hence, ensuring the principal angles remain unchanged is one option for maintaining some useful properties. Specifically,

for any two pairs of subspaces (A,B) and (C,D), if the principal angles of (A,B) and (C,D) are the same (implying that $\min\{\dim(A),\dim(B)\}=\min\{\dim(C),\dim(D)\},\dim(A)$ represents the dimension of A), then relationship between A and B can be regarded as similar to the relationship between C and D. Based on this idea, the definition of measurement D, which describes the relationships between two pairs of subspaces, follows.

Definition 4 (measurement between subspace pairs). Given two pairs of subspaces (A, B) and (C, D), the measurement $\mathcal{D}((A, B), (C, D))$ between (A, B) and (C, D) is defined as

$$\mathcal{D}((A,B),(C,D)) = \sum_{i=1}^{r} \left| \sigma_i(A^T B) - \sigma_i(C^T D) \right|, \quad (6)$$

where A, B, C and D are subspaces in \mathbb{R}^N , $r=\min\{\dim(A), \dim(B), \dim(C), \dim(D)\}$ and $\sigma_i(A^TB)$ is the i^{th} singular value of matrix A^TB and represents cosine value of the i^{th} principal angle between A and B.

Measurement \mathcal{D} defined on $G_{N,*}^T \times G_{N,*}$ is actually a metric, as proven in the following theorem.

Theorem 3. $(\mathcal{D}, G_{N,*}^T \times G_{N,*})$ is a metric space, where $G_{N,*} = \{A | A \in G_{N,i}, \ i = 1, ..., N-1\}.$

Proof. Let A, B, C, D, E and F are subspaces in \mathbb{R}^N . Thus, we need to prove following conditions.

- 1) $\mathcal{D}((A, B), (C, D)) \ge 0$;
- 2) $\mathcal{D}((A, B), (C, D)) = \mathcal{D}((C, D), (A, B));$
- 3) $\mathcal{D}((A,B),(C,D)) = 0 \Leftrightarrow A^TB = C^TD;$
- 4) $\mathcal{D}((A,B),(C,D)) \leq \mathcal{D}((A,B),(E,F)) + \mathcal{D}((E,F),(C,D)).$

From Definition 4, it is easy to prove 1) and 2). Based on Definition 3 (principal angles for heterogeneous feature spaces), we know $\sigma_i(A^TB) = \sigma_i(C^TD) \Leftrightarrow A^TB = C^TD$, which means that $\sigma_i(A^TB) - \sigma_i(C^TD) = 0 \Leftrightarrow A^TB = C^TD$. Therefore, 3) is also proven. For 4), we have

$$\mathcal{D}((A,B),(C,D))$$

$$= \sum_{i=1}^{r} \left| \sigma_i(A^T B) - \sigma_i(E^T F) + \sigma_i(E^T F) - \sigma_i(C^T D) \right|$$

$$\leq \sum_{i=1}^{r} \left| \sigma_i(A^T B) - \sigma_i(E^T F) \right| + \sum_{i=1}^{r} \left| \sigma_i(E^T F) - \sigma_i(C^T D) \right|$$
$$= \mathcal{D}((A, B), (E, F)) + \mathcal{D}((E, F), (C, D)).$$

Thus, condition 4) is proven and
$$(\mathcal{D}, G_{N,*}^T \times G_{N,*})$$
 is a metric

space.

The definition of the consistency of the geometry relation with respect to feature spaces of two domains can be given in terms of the metric \mathcal{D} as follows.

Definition 5 (consistency of the geometry relation). Given the source domain $\mathbf{D_s} = (X_s, Y_s)$ and the heterogeneous and unlabeled target domain $\mathbf{D_s} = (X_t)$, let $f_s(X_s) = X_s U_s^T$ and $f_t(X_t) = X_t U_t^T$, if $\forall \delta \in (0, \delta_0]$, $\exists \epsilon < \mathcal{O}(\delta_0)$ such that

$$\int_0^{\delta_0} \mathcal{D}\Big((S_{X_s^{\delta}}, S_{X_t^{\delta}}), (S_m(f_s, X_s^{\delta}), S_m(f_t, X_t^{\delta}) \Big) d\delta < \epsilon, \tag{7}$$

then we can say (X_s, X_t) and $(f_s(X_s), f_t(X_t))$ have consistent geometry relations, where $S_{X^\delta} = span(X + \delta \cdot \mathbf{I}_X)$, $S_m(f, X^\delta) = span(f(X + \delta \cdot \mathbf{I}_X))$, $U_s \in \mathbb{R}^{r \times m}$, $U_t \in \mathbb{R}^{r \times n}$, $r = min\{m, n\}$ and \mathbf{I}_X is a matrix of ones of the same size as X.

This definition precisely demonstrates how f_s and f_t influence the geometric relation between the original feature spaces and the feature spaces of homogeneous representations. If there are slight changes in the original feature spaces, we hope the feature spaces of the homogeneous representations will also see slight changes. If they do, it means that the feature spaces of the homogeneous representations are consistent with the geometry relations of the two original feature spaces. If we use definitions of D_{He} and D_{Ho} , (7) can be expressed by

$$\int_{0}^{\delta_{0}} \mathcal{D}\left((S_{X_{s}^{\delta}}, S_{X_{t}^{\delta}}), (S_{m}(f_{s}, X_{s}^{\delta}), S_{m}(f_{t}, X_{t}^{\delta})\right) d\delta < \epsilon$$

$$\Leftrightarrow \int_{0}^{\delta_{0}} \left\|D_{He}(X_{s}^{\delta}, X_{t}^{\delta}) - D_{Ho}(f_{s}(X_{s}^{\delta}), f_{t}(X_{t}^{\delta}))\right\|_{\ell_{1}} d\delta < \epsilon.$$
(8)

To ensure the consistency of the geometric relation of the two original feature spaces, we can minimize following cost function to ensure we are able to find an ϵ that is less than $\mathcal{O}(\delta_0)$, such that $\int_0^{\delta_0} \mathcal{D}\big((S_{X_s^\delta},S_{X_t^\delta}),(S_m(f_s,X_s^\delta),S_m(f_t,X_t^\delta)\big)d\delta < \epsilon$ when there are slight changes $\delta \in (0,\delta_0]$ in the original feature spaces.

Definition 6 (cost function I). Given the source domain $\mathbf{D_s} = (X_s, Y_s)$ and the heterogeneous and unlabeled target domain $\mathbf{D_s} = (X_t)$, let $f_s(X_s) = X_s U_s^T$ and $f_t(X_t) = X_t U_t^T$, the cost function J_1 of GLG is defined as

$$J_{1}(X_{s}, X_{t}; U_{s}, U_{t})$$

$$= \int_{0}^{\delta_{0}} \|D_{He}(X_{s}^{\delta}, X_{t}^{\delta}) - D_{Ho}(X_{s}^{\delta}, X_{t}^{\delta})\|_{\ell_{1}} d\delta$$

$$+ \frac{1}{2} \lambda_{s} Tr(U_{s} U_{s}^{T}) + \frac{1}{2} \lambda_{t} Tr(U_{t} U_{t}^{T}), \tag{9}$$

where $X^{\delta} = X + \delta \cdot \mathbf{1}_{X}$, $U_{s} \in \mathbb{R}^{r \times m}$, $U_{t} \in \mathbb{R}^{r \times n}$, $r = min\{m,n\}$ and $\mathbf{1}_{X}$ is a matrix of ones of the same size as X.

This definition shows the divergence between the original feature spaces and the feature spaces of the homogeneous representations via principal angles. If we use $\theta_i^{(o)}$ to represent the i^{th} principal angle of the original feature spaces and $\theta_i^{(m)}$ to represent the i^{th} principal angle of the feature spaces of the homogeneous representations, J_1 measures the divergence of $|cos(\theta_i^{(o)}) - cos(\theta_i^{(m)})|$ when the original feature spaces have slight changes. $Trace(U_sU_s^T)$ and $trace(U_tU_t^T)$ are used to smooth f_s and f_t . λ_s is set to 0.01/mr, and λ_t is set to 0.01/mr. When m=n, λ_s and λ_t are set to 0. From Definition 6, it is obvious that the maps $f_s(X_s)$ and $f_t(X_t)$ will ensure all principal angles slightly change as J_1 approaches 0, even when there is some disturbance of up to δ_0 . Thus, based on Theorem 2 and Definition 6, the GLG model is presented follows.

Model (GLG). The model GLG aims to find $U_s \in \mathbb{R}^{r \times m}$, $U_t \in \mathbb{R}^{r \times n}$ to minimize the cost function J_1 , as defined in (9), while $f_s(X_s) = X_s U_s^T$ and $f_t(X_t) = X_t U_t^T$ are LMMs. GLG is expressed as

$$\begin{split} & \underset{U_s,U_t}{\text{Min}} \quad J_1(X_s,X_t;U_s,U_t) \\ & s.\ t. \quad U_s>0 \quad \text{and} \quad U_t>0. \end{split}$$

 $f_s(X_s)$ and $f_t(X_t)$ are the new instances corresponding to X_s and X_t in the homogeneous representations with a dimension of r. Knowledge is then transferred between $f_s(X_s)$ and $f_t(X_t)$ using GFK. Figure 1 illustrates GLG's process.

Admittedly, LMMs are somewhat restrictive map because all elements in the U must be positive numbers. However, we use LMMs to prevent negative transfers that can significantly reduce prediction accuracy in the target domain. From the perspective of the entire transfer process, an LMM, as a positive map, is the only map that can help construct the homogeneous representations ($V_{He} = V_{Ho}$ and $D_{He} = D_{Ho}$). The GFK model provides the second map, which does not have such rigid restrictions and makes $V_{Ho} < V_{He}$ and $D_{Ho} < D_{He}$. Hence, the composite map (LMM+GFK) does not carry rigid restrictions and can therefore handle more complex problems. LMMs ensure correctness, thus avoiding negative transfer, and the GFK model (or another HoUDA model developed in future work) improves the ability to transfer knowledge. Following theorem demonstrates that GFK is a degenerate of the GLG model.

Theorem 4 (degeneracy of GLG). Given the source domain $\mathbf{D_s} = (X_s, Y_s)$ and the heterogeneous and unlabeled target domain $\mathbf{D_s} = (X_t)$, if two domains are homogeneous (m = n), then the GLG model degenerates into the GFK model.

Proof. Proving this theorem only requires proving that the optimized U_s^* and U_t^* in the GLG model are identical matrixes when m=n. In terms of Theorem 3, it is obvious that $\mathcal{D}((S_{X_s^\delta},S_{X_t^\delta}),(S_{X_s^\delta},S_{X_t^\delta}))=0$. So, if $f_s(X_s)=X_s$ and $f_t(X_t)=X_t$, then we have $J_1=0$ (when $m=n,\lambda_s=\lambda_t=0$), which results in the optimal GLG model.

Because $f_s(X_s) = X_s \Leftrightarrow U_s = I_s$ and $f_t(X_t) = X_t \Leftrightarrow U_t = I_t$, the GLG model degenerate into an ordinary GFK model.

Since this optimization issue is related to the subspaces spanned by the original instances $(X_s \text{ and } X_t)$ and the subspaces spanned by the distributed instances $(X_s^\delta \text{ and } X_t^\delta)$, the best way to efficiently arrive at an optimized solution is a difficult and complex problem. Section IV proposes the optimization algorithm, focusing on the solution for GLG.

IV. OPTIMIZATION OF GLG

According to (9), we need to calculate 1) $\partial \sigma_i(C^TD)/\partial U_s$, $\partial \sigma_i(C^TD)/\partial U_t$ and 2) the integration with respective to δ to minimize J_1 via a gradient decent algorithm, where $C = span(f_s(X_s^\delta)), \ D = span(f_t(X_t^\delta)), \ \delta \in (0, \delta_0]$ and i = 1, ..., r. Because deriving $\partial \sigma_i(C^TD)/\partial U_s$ and $\partial \sigma_i(C^TD)/\partial U_t$ contains the process of spanning a feature

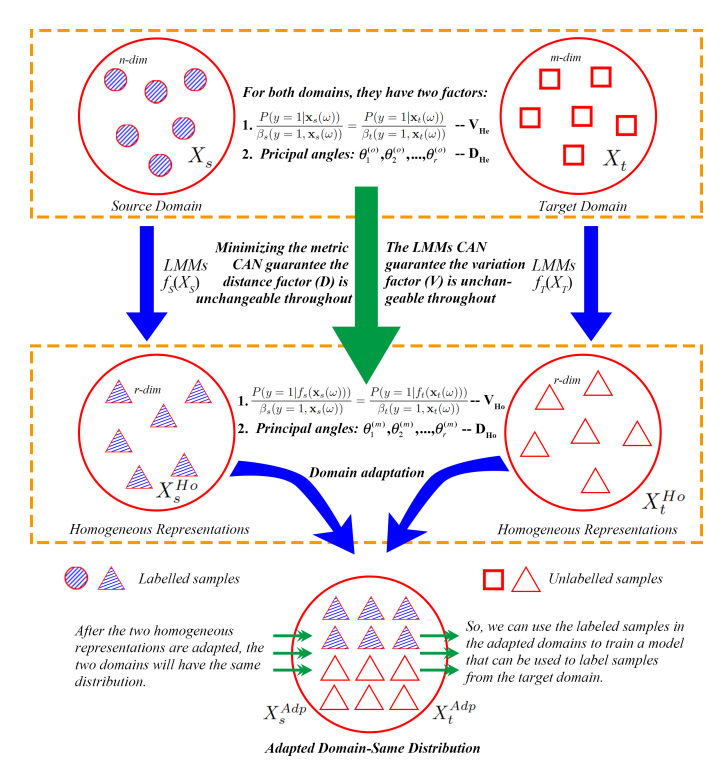


Fig. 1: The progress of the GLG model. For original source and target domains, two factors are used to describe the similarity between two domains, V_{He} and D_{He} . Hence, we hope two homogeneous representations have the same similarity with original ones. The LMMs can guarantee the variation factor unchangeable and minimizing J_1 can guarantee the distance factor unchangeable. After constructing homogeneous representations, GFK is applied to transfer knowledge across domains.

space to be a subspace. Thus, when there are some disturbances in an original feature space, the microscopic changes of the eigenvectors in an Eigen dynamic system (EDS) need to be analyzed (Eigenvectors are used to construct the subspaces spanned by a feature space, i.e., C and D). The following subsection discusses the microscopic analysis of an Eigen dynamic system.

A. Microscopic analysis of an Eigen dynamic system

In this section, we explore the extent of the changes in subspace A = span(X) when the feature space (X) has suffers a disturbance, expressed as $\partial A/\partial X$. Without loss of generality, assume $A \in G_{N,n}$ (formed as an $\mathbb{R}^{N \times n}$ matrix) and $X \in \mathbb{R}^{N \times n}$, where n is the number of features of X and X is the dimension of the whole space. In keeping with SVD, X is the first X columns of the eigenvectors of X is the first X columns of the eigenvectors of X is the first X columns of the eigenvectors of X is the following equations:

$$XX^T y_i = y_i \lambda_i, \ i = 1, ..., n$$
$$y_i^T y_i = 1,$$

where y_i is the i^{th} column of A, and λ_i is the eigenvalue corresponding to y_i .

It is obvious that if X is disturbed due to equality, y_i and λ_i will change correspondingly. This equation represents a basic EDS, which is widely used in many fields. To microscopically analyze this equation, we differentiate it into

$$\frac{\partial XX^T}{\partial X}y_i + XX^T \frac{\partial y_i}{\partial X} = y_i \frac{\partial \lambda_i}{\partial X} + \frac{\partial y_i}{\partial X} \lambda_i.$$
 (10)

After a series of calculations, Lemma 2 is derived as follows.

Lemma 2 (first-order derivatives of EDS). Given a feature space $X \in \mathbb{R}^{N \times n}$, let $A = span(X) \in G_{N,n}$ (formed as an $\mathbb{R}^{N \times n}$ matrix), let y_i be the i^{th} column of A, and let λ_i be the eigenvalue corresponding to y_i . The first-order derivatives of the EDS are

$$\frac{\partial y_i}{\partial X} = -(XX^T - \lambda_i I)^+ \frac{\partial XX^T}{\partial X} y_i,$$
$$\frac{\partial \lambda_i}{\partial X} = y_i^T \frac{\partial XX^T}{\partial X} y_i,$$

where $(XX^T - \lambda_i I)^+$ is the Moore-Penrose pseudoinverse of $XX^T - \lambda_i I$.

Proof. Let 1) Λ represent the diagonal matrix constructed by λ_i ; 2) $(XX^T - \lambda_i I)^- = A(\Lambda - \lambda_i I)^+ A^T$; and 3) $e_i = A^{-1}y_i$. Hence, we derive the following equations:

$$XX^{T}A = A\Lambda, \ (\Lambda - \lambda_{i}I)^{-}e_{i} = (\Lambda - \lambda_{i}I)^{-}e_{i} = 0,$$

$$(XX^{T} - \lambda_{i}I)^{-}(XX^{T} - \lambda_{i}I)(XX^{T} - \lambda_{i}I)^{-} = (XX^{T} - \lambda_{i}I)^{-},$$

$$(XX^{T} - \lambda_{i}I)(XX^{T} - \lambda_{i}I)^{-}(XX^{T} - \lambda_{i}I) = (XX^{T} - \lambda_{i}I).$$

Based on these equations and $(XX^T - \lambda_i I)^- = A(\Lambda - \lambda_i I)^+ A^T$, we obtain

$$(XX^T - \lambda_i I)^- (XX^T - \lambda_i I) = I - y_i y_i^T, \qquad (11)$$

$$(XX^T - \lambda_i I)^- y_i = 0. (12)$$

Next, we calculate the first-order derivatives of the EDS. First, we transform (10) into the following term.

$$(XX^{T} - \lambda_{i}I)\frac{\partial y_{i}}{\partial X} = y_{i}\frac{\partial \lambda_{i}}{\partial X} - \frac{\partial XX^{T}}{\partial X}y_{i}.$$
 (13)

Then, we pre-multiply both sides of $(XX^T - \lambda_i I)^-$ and arrive at the following equation based on (11).

$$(I - y_i y_i^T) \frac{\partial y_i}{\partial X} = (XX^T - \lambda_i I)^T y_i \frac{\partial \lambda_i}{\partial X} - (XX^T - \lambda_i I)^T \frac{\partial XX^T}{\partial X} y_i.$$

Due to (12), we have

$$\frac{\partial y_i}{\partial X} - y_i y_i^T \frac{\partial y_i}{\partial X} = -(XX^T - \lambda_i I)^{-1} \frac{\partial XX^T}{\partial X} y_i.$$
 (14)

Since $y_i^T y_i = 1$, we arrive at

$$\frac{\partial y_i^T}{\partial X} y_i + \frac{\partial y_i}{\partial X} y_i^T = 0 \Rightarrow y_i^T \frac{\partial y_i}{\partial X} = 0.$$
 (15)

Hence, we arrive at the derivatives of the eigenvector.

$$\frac{\partial y_i}{\partial X} = -(XX^T - \lambda_i I)^+ \frac{\partial XX^T}{\partial X} y_i.$$

We only need to pre-multiply both sides of (13) with y_i^T to calculate the derivatives of the eigenvalue,

$$\frac{\partial \lambda_i}{\partial X} = y_i^T \frac{\partial X X^T}{\partial X} y_i.$$

This lemma is proven

Based on Lemma 2, we know the extent of the changes in subspace A = span(X) when the feature space (X) has suffers a disturbance, expressed as $\partial A/\partial X$.

B. Gradients of J_1

With the proposed lemma, we obtain the derivative of cost function J_1 using following chain rules. For simplicity, S_m^s is short for $S_m(f_s, X_s^\delta)$ and S_m^t is short for $S_m(f_t, X_s^\delta)$.

$$\frac{\partial J_1}{\partial (U_s)_{cd}} = \int_{\delta=0}^{\delta_0} \frac{\partial J_1}{\partial \mathcal{D}} \sum_{i=1}^r \frac{\partial \mathcal{D}}{(\partial \sigma_i((S_m^s)^T S_m^t))} \cdot Tr\left(\left(\frac{\partial \sigma_i((S_m^s)^T S_m^t)}{\partial S_m^s}\right)^T \frac{\partial S_m^s}{\partial (U_s)_{cd}}\right) d\delta + \lambda_s(U_s)_{cd}.$$
(16)

The first and second terms of the right side can be easily calculated according to the definition of the cost function J_1 . Using chain rules, the third term can be calculated by the following equations:

$$\frac{\partial \sigma_i((S_m^s)^T S_m^t)}{\partial (S_m^S)_{kl}} = Tr\left(\left(\frac{\partial \sigma_i((S_m^s)^T S_m^t)}{\partial (S_m^s)^T S_m^s}\right)^T \frac{\partial (S_m^s)^T S_m^s}{\partial (S_m^S)_{kl}}\right),\tag{17}$$

$$\frac{\partial(S_m^S)_{kl}}{\partial(U_s)_{cd}} = Tr\left(\left(\frac{\partial(S_m^s)_{kl}}{\partial f_s(X_s^\delta)}\right)^T \frac{\partial f_s(X_s^\delta)}{\partial(U_s)_{cd}}\right). \tag{18}$$

In terms of the first-order derivatives of EDS, we have following equations:

$$\left(\frac{\partial \sigma_{i}((S_{m}^{s})^{T}S_{m}^{t})}{\partial (S_{m}^{s})^{T}S_{m}^{s}}\right)_{pq} = \frac{1}{2\sigma_{i}((S_{m}^{s})^{T}S_{m}^{t})} y_{i}^{T} \left(J_{pq}((S_{m}^{s})^{T}S_{m}^{t})^{T} + ((S_{m}^{s})^{T}S_{m}^{t})J_{pq}^{T}\right) y_{i}, \tag{19}$$

$$\left(\frac{\partial (S_m^s)_{kl}}{\partial f_s(X_s^{\delta})}\right) = -\left((f_s(f_s)^T - \lambda_l I)^+ (J_{ab}(f_s)^T + f_s J_{ab}^T) \cdot (S_m^s)_{*l}\right)_k,$$
(20)

where y_i is the eigenvector corresponding to $\sigma_i((S_m^s)^T S_m^t)$, λ_l is the l^{th} eigenvalue corresponding to l^{th} column of S_m^s , and J_{pq} is a single-entry matrix with 1 at (p;q) and zero elsewhere. (19) will generate a matrix of the same size as $(S_m^s)^T S_m^t$, and (20) will generate a matrix of the same size as $f_s(X_s^\delta)$, i.e., f_s in (20). For other terms of (17) and (18), we have following equations:

$$\frac{\partial (S_m^s)^T S_m^s}{\partial (S_m^s)_{kl}} = J_{kl}^T S_m^t + (S_m^s)^T J_{kl},\tag{21}$$

$$\frac{\partial f_s(X_s^{\delta})}{\partial (U_s)_{cd}} = X_s^{\delta} J_{cd}.$$
 (22)

We adopt Simpson's rule to integrate δ . Simpson's rule is a method of numerical integration that can be used to calculate the value of cost function J1. We set $\Delta = \delta_0/10$, and the derivative of cost function J_1 is calculated with

$$\frac{\partial J_1}{\partial (U_s)_{cd}} = \frac{\Delta}{6} \sum_{I=0}^{9} \left(g_s(I\Delta) + 4g_s(I\Delta + \frac{\Delta}{2}) + g_s(I\Delta + \Delta) \right) + \lambda_s(U_s)_{cd}, \tag{23}$$

where $g_s(\Delta)$ is the integrated part in (16) with $S_m^s = S_m(f_s, X_s^{\Delta})$. The gradient decent equations for minimizing the cost function J_1 with respect to $(U_s)_{cd}$ are

$$(U_s)_{cd} = (U_s)_{cd} - v_{bool}^s \times \eta \frac{\partial J_1}{\partial (U_s)_{cd}}, \tag{24}$$

where

$$v_{bool}^{s} = max \Big\{ 0, (U_s)_{cd} - \eta \frac{\partial J_1}{\partial (U_s)_{cd}} \Big\}, \tag{25}$$

 v_{bool}^s , expressed in (25), is used to constrain f_s is LMMs. Similarly, we optimize U_t using a following equation.

$$(U_t)_{ce} = (U_t)_{ce} - v_{bool}^t \times \eta \frac{\partial J_1}{\partial (U_t)_{ce}}.$$
 (26)

C. Optimization of GLG

We use a hybrid way to minimizing J_1 : 1) an evolutionary algorithm: cuckoo search algorithm (CSA) [48], is used to find initial solutions $U_s^{(0)}$ and $U_t^{(0)}$; 2) an gradient decent algorithm to find the best solutions. To accelerate the speed of the gradient decent algorithm, we select η from [0.01, 0.05 0.1, 0.2, 0.5, 1, 5, 20] such that it obtains the best (minimum) cost value for each iteration.

For CSA, we set the number of nests as 30, discovery rate as 0.25, lowest bound as 0, highest bound as 1 and number of iteration as 100. We also apply the Simpson's rule to estimate the integration value in J_1 . CSA has been widely applied in many fields. Its code can be downloaded from MathWorks.com where readers can also find more detailed information about this algorithm. Algorithm 1 presents the pseudo code of GLG model. MaxIter is set to 100, err is set to 10^{-5} and δ_0 of J_1 is set to 0.01.

Ultimately, $\mathbf{D}_s^{Adp}=(X_s^{Adp},Y_s)$ can be used to train a machine learning model, based on X_s^{Adp} and X_t^{Adp} , to predict the labels for $\mathbf{D}_t^{Adp}=(X_t^{Adp})$.

V. EXPERIMENTS

To validate the overall effectiveness of the GLG model, we conducted extensive experiments with five datasets across three fields of application: cancer detection, credit assessment, and text classification. All datasets are publicly available from the UCI Machine Learning Repository (UMLR) and Transfer Learning Resources (TLR). An SVM algorithm was used as the classification engine.

Algorithm 1: Pseudo code of GLG model

A. Datasets for HeUDA

The five datasets were reorganized since no public datasets directly relate to HeUTL. Table I lists the details of the datasets as sourced from UMLR and TLR. Reuters-21578 is a transfer learning dataset, but we needed to merge the source domain for each category with its corresponding target domain into a new domain e.g., OrgsPeople_src and OrgPeople_tar were merged into OrgPeople; and similarly for OrgPlaces and PeoplePlaces. Table II lists the transfer tasks and clarifies the source and target domains. Tasks G2A, Ope2Opl and CO2CD are described in detail below. Other tasks have similar meanings.

- 1) G2A: Assume that the German data is labeled and the Australian data is unlabeled. Label "1" means good credit and label "-1" means bad credit. This task is equivalent to the question: "Can we use knowledge from German credit records to label unlabeled Australian data?"
- 2) Ope2Opl: Assume that in one dataset Org is labeled "1" and People is labeled "-1" (Ope in Table II). Another unlabeled dataset may contain Org labeled as "1". This task is equivalent to the question: "Can we use the knowledge from Ope to label "Org" in the unlabeled dataset?"
- 3) CO2CD: Assume that in the Breast Cancer Wisconsin (Original) dataset (CO in Table II) "1" represents malignant and "-1" represents benign. Another unlabeled dataset related to breast cancer also exists. This task is equivalent to the question: "Can we use the knowledge from CO to label "malignant" in the unlabeled dataset?"

B. Experimental setup

The baseline models we compared GLG to, along with their implementation details, are described in the following section.

1) Baseline models: It was important to consider which benchmarks to compare the GLG model with. There are two baselines that naturally consider situations where no related knowledge exists in an unlabeled target domain: 1) models that label all instances as 1, denoted as A1; and 2) models that cluster the instances with random category labels (the k-means method clusters the instances in the target domain into

two categories), denoted as CM. It is important to highlight that A1 and CM are non-transfer models.

When using knowledge from a source domain, there is a simple benchmark model that applies dimensional reduction technology to force the two domains to have the same number of features. Denoted as Dimensional reduction Geodesic flow kernel (DG), this model reduces the dimensionality of all feature spaces to the dimensionality of the lowest dimensional feature spaces. Although the DG model does not guarantee that two lower dimensional feature spaces will retain their similarity, it is still a useful model for showing the difficulties associated with HeUDA. An alternative model, denoted as Random Maps GFK (RMG), randomly maps (linear map) two domains onto the same dimensional space. The comparison between this model and Random LMM GFK (RLG) shows the effect of negative transfer. The RLG model only uses random LMMs to construct the homogeneous representations and does not preserve the distance between the domains (it only considers the variation factor). KCCA model with random paired instances is also considered as a baseline model to show ability of GLG model when there is no paired instances across two heterogeneous domains. All KCCA, DG, RMG, RLG, and GLG models are able to map two heterogeneous feature spaces onto the same dimensional feature space (i.e., the homogeneous representations) at the lowest dimension of the original feature spaces.

2) Implementation details: Following [1], [38], [28], [39], SVM was trained on the homogeneous representations of the source data, then tested on the unlabeled target data. The following section provides the implementation details for the four experiments we conducted. We compare RMG model to CM model in the first experiment and shows the negative effects caused by negative transfer. In the second experiment, RLG model is compared to CM model. This experiment presents that the significance of the unsupervised knowledge transfer theorem. GLG model is tested in the third experiment and compared to CM model. In the fourth experiment, classification results of A1, CM, DG, KCCA, RMG, RLG and GLG are presented.

The original datasets used in the text classification tasks were preprocessed using SVD (selecting top 50% Eigenvalues) as the dimensionality reduction method, and we randomly selected 1500 unbiased instances from each domain to test the proposed model and baselines. Additionally, the order of features and instances in each dataset were randomly permuted before knowledge transfer. The German Credit dataset contains some bias, with 70% of the dataset labeled 1 and 30% labeled -1; however, the Australian Credit Approval dataset is unbiased. Given the basic assumption that both domains are similar, we needed to offset this dissimilarity by changing the implementation of the experiments with this dataset. Hence, we randomly selected 600 unbiased instances from the German Credit dataset for every experiment and ran the experiment 50 times for each model and each task.

Since the target domains do not contain any labeled data, it was impossible to automatically tune the optimal parameters for the target classifier using cross-validation. As a result, we used LIBSVMs default parameters for all classification tasks:

TABLE I: Description of the original datasets.

Field	Dataset name	# of instances	# of features	Source
	German Credit Data	1000	24	UMLR
Credit assessment (two datasets)	Australian Credit Approval	690	14	UMLR
	Reuters-21578 OrgsPeople_src	1237	4771	TLR
	Reuters-21578 OrgsPeople_tar	1208	4771	TLR
Taxt alassification (and dataset)	Reuters-21578 OrgsPlaces_src	1016	4415	TLR
Text classification (one dataset)	Reuters-21578 OrgsPlaces_tar	1043	4415	TLR
	Reuters-21578 PeoplePlaces_src	1077	4562	TLR
	Reuters-21578 PeoplePlaces_tar	1077	4562	TLR
	Breast Cancer Wisconsin (Original)	683	9	UMLR
Cancer detection (two datasets)	Breast Cancer Wisconsin (Diagnostic)	569	30	UMLR

TABLE II: Transfer tasks (10 tasks in total).

Field	Source	Target	Labels	Task
	German Credit Data	Australian Credit Approval	1: Good	G2A
Credit assessment (two datasets)	Australian Credit Approval	German Credit Data	1: Good	A2G
	OrgsPeople	OrgsPlaces	1: Orgs	Ope2Opl
	OrgsPlaces	OrgsPeople	1: Orgs	Opl2Ope
Text classification (one dataset)	OrgsPlaces	PeoplePlaces	-1: Places	Opl2Ppl
Text classification (one dataset)	PeoplePlaces	OrgsPlaces	-1: Places	Ppl2Opl
	PeoplePlaces	OrgsPeople	-	Ppl2Ope
	OrgsPeople	PeoplePlaces	-	Ope2Ppl
	Breast Cancer Wisconsin (Original)	Breast Cancer Wisconsin (Diagnostic)	1: Malignant	CO2CD
Cancer detection (two datasets)	Breast Cancer Wisconsin (Diagnostic)	Breast Cancer Wisconsin (Original)	1: Malignant	CD2CO

TABLE III: Same-domain accuracy of each target domain using 5-fold SVM.

German	Australia	Opl	Ope	Ppl	CD	CD
71.21% ±1.56%	$86.10\% \pm 0.82\%$	84.97% ±0.88%	85.15% ±0.71%	$78.40\% \pm 0.82\%$	$97.01\% \pm 0.00\%$	96.49% ±0.00%

the of the radial basis function kernel was set to 1/r (where r is the dimension of the feature space of the homogeneous representations); the cost C was set to 1; and the tolerance of the termination criterion was set to 0.001. Because there were no existing pairs for the 10 transfer learning tasks, we randomly matched instances from each domain as pairs for the KCCA model.

Accuracy was used as the test metric as it has been widely adopted in the literature [28], [17], [38]. The definition follows.

$$Accuracy = \frac{|x \in X_t : g(x) = y(x)|}{|x \in X_t|},$$

where y(x) is the ground truth label of x, while g(x) is the label predicted by the SVM classification algorithm. All experiments were conducted on an Intel(R) Core(TM) i7-4770 CPU at 3.40Ghz with a memory of 64 GB running Windows 7 professional 64-bit operating system and Matlab 9.2.0. To show the complexity of each task, we also tested same-domain accuracy with a 5-fold SVM using the default parameters on seven different target domains. We randomly selected unbiased instances from five domains (the cancer datasets were excluded), and ran the experiments 50 times, preprocessing the instances with the zscore function. Table III shows the average accuracy and standard deviations in terms of AVG \pm STD. The results show that the German Credit dataset and the Ppl dataset were the hardest to classify and the

Cancer-D and Cancer-O datasets were the easiest. In general, the accuracy of the HeUDA models was lower than the samedomain (target) accuracy due to the lack of labels in the target domain.

C. Experiment I: RMG

This experiment demonstrates a situation where the transfer process is unreliable. It is a natural idea to propose an HeUDA model that randomly maps two domains onto the same feature space, then uses an HoUDA model to adapt the domains. Hence, the RMG model randomly generated $f_s(X_s) = X_s U_s^T$ and $f_t(X_t) = X_t U_t^T$ to transfer knowledge from the source domain to the target domain. Table IV shows the classification results for RMG compared to CM across 50 tests against three criteria: AVG \pm STD, max accuracy, and min accuracy. The results indicate that RMG is not a valid option for transferring knowledge from a source domain to a target domain. The accuracy across 50 tests was low, especially for the CD2CO task, where the minimum accuracy was 7.91%. This means the label space was greatly changed during the knowledge transfer.

The results of the two-sample MMD tests [29] are shown in Table V to demonstrate the significance of Theorem 1. These tests measure the maximum and minimum accuracy of the homogeneous representations for the two CD2CO tasks. In Table V, No means that the two domains have different distributions; Yes means the two domains have the same distribution. It is easy to see that distributions of feature spaces of adapted domains can be regarded as having the same distribution (in terms of MMD) in these two extreme situations (highest and lowest accuracy). However, these identically-distributed domains unexpectedly resulted in extremely different accuracies at 7.91% and 96.49% when using SVM to label the instances in the target domain. This will result in significant errors even if $P(f_s(X_s)) = P(f_t(X_t))$, which is obviously caused

		Average Accuracy	Average Accuracy Max A		ax Accuracy		Min Accuracy	
Field	Task	RMG	CM	RMG	CM	RMG	CM	
	G2A	49.46%±13.31%	44.89%±0.40%	75.94%	56.23%	24.49%	43.77%	
Credit Assessment (Two datasets)	A2G	$49.34\% \pm 5.2\%$	$50.97\% \pm 5.21\%$	59.33%	57.17%	36.00%	43.67%	
	OPe2OPl	$52.36\% \pm 5.20\%$	$49.76\% \pm 5.79\%$	62.47%	59.93%	41.27%	40.07%	
	OP12OPe	$46.14\% \pm 5.10\%$	$49.4\% \pm 5.01\%$	56.00%	56.87%	37.33%	43.13%	
T (C) (C) (O) 1 (O)	OP12PP1	$48.98\% \pm 5.84\%$	$50.70\% \pm 5.24\%$	62.67%	58.40%	36.13%	41.47%	
Text Classification (One dataset)	PP12OP1	$49.34\% \pm 5.58\%$	$49.76\% \pm 5.79\%$	64.27%	59.93%	38.40%	40.07%	
	OPe2PPl	$51.83\% \pm 4.99\%$	$50.70\% \pm 5.24\%$	60.80%	58.40%	40.07%	41.47%	
	PP12OPe	$49.35\% \pm 4.88\%$	$49.4\% \pm 5.01\%$	61.40%	56.87%	40.47%	43.13%	
	CD2CO	$58.92\% \pm 27.88\%$	$38.94\% \pm 45.17\%$	96.49%	96.19%	7.91%	3.81%	
Cancer Detection (Two datasets)	CO2CD	$49.18\%\!\pm\!20.87\%$	$37.25\% \pm 33.37\%$	89.10%	85.41%	14.41%	14.59%	

TABLE IV: The classification results for RMG and CM.

by $P(Y|f_s(X_s)) \neq P(Y|f_t(X_t))$ (significant difference). Thus, this experiment supports our claim that Definition 1 (the HeUDA condition) and Theorem 1 (the unsupervised knowledge transfer theorem) are both necessary. It also shows the consequences of ignoring Theorem 1 - the conditional probability distribution will significant change.

TABLE V: The results of the MMD test for the mapped and adapted domains in two extreme situations (lowest and highest accuracy) of task CD2CO among 50-time experiments.

Situation	Task/Accuracy	Homogeneous representations	Adapted domains
Lowest Accuracy	CD2CO/7.91%	No	Yes
Highest Accuracy	CD2CO/96.49%	No	Yes

D. Experiment II: RLG

This experiment demonstrates the classification results for RLG and CM. LMM is a suitable map choice for Theorem 1, because LMMs can guarantee that the conditional probability distribution will not significantly change during knowledge transfer. Table VI lists the classification results of this experiment across 50 tests against three criteria: AVG±STD, max accuracy, and min accuracy.

From Table VI, it is clear that RLG is better than CM and RMG. Notably, in the cancer detection tasks, RLG showed a much higher average accuracy with levels above 90%. Several observations can be made from the overall results.

- 1) RLGs effectiveness is significantly different for datasets from different fields;
- 2) Using knowledge from the German credit records to help classify Australian data was more effective than the other way around (A2G). There are two probable reasons: a) the German data has a greater number of features that express similar meanings in the Australian data; and b) the Australian data are easier to label than German data in terms of same-domain accuracy;
- 3) On the Ope dataset, the knowledge transfer was better from Opl than Ppl. This may be because Ope is directly related to Opl and Ppl is not;
- 4) On the Ppl dataset, the knowledge transfer was better from Opl than Ope. Again, Ppl is directly related to Opl and Ope is not;

- 5) Using knowledge from the CD data to help classify CO data was more effective than CO2CD, which may be because the CD data has more features that express similar meanings in the CO data;
- 6) The RLG model performed more effectively than CM and RMG across every evaluation criteria.

These overall results reflect that the proposed LMMs and Theorem 1 are significant findings for HeUTL models.

E. Experiment III: GLG

The experiments in this section demonstrate the comparison between GLG and CM. The classification results across 50 tests against three criteria, AVG±STD, max accuracy, and min accuracy are listed in Table VII. From Table VII, it is clear that GLG is better than CM and RMG. Again, GLG showed much higher average accuracy in the field of cancer detection with levels above 90%. The overall results reveal similar observations as the classification results for RLG and CM in Table VI.

F. Experiment IV: Overall comparisons

Having separately tested CM, RMG, RLG, and GLG, this section combines the classification results and compares them to A1, DG, and KCCA as shown in Table VIII. The results reflect that the RLG and GLG model were able to complete these 10 tasks effectively, and with better accuracy than other benchmarks. Our overall analysis of the comparative results reveals the following insights:

- 1) The GLG model produced more stable classification results than the other models across 50 experiments;
- 2) The GLG and RLG models show higher classification accuracy than the other models across 50 experiments;
- 3) The A1 model outperformed the other models in most tasks because the DG, CM, and RMG models do not guarantee that the label space will remain unchanged during knowledge transfer;
- 4) Although the KCCA model outperformed A1, DG, CM, and RMG in some tasks, the classification results were unstable as KCCA does not prevent negative transfer;
- 5) Given the same target domain, the source domain selected influences the classification results;
- 6) In comparing same-domain accuracy, the CD2CO task outperformed the CO task. Same-domain accuracy was harder

 $57.71\% \pm 2.50\%$

 $63.07\% \pm 3.11\%$

 $56.88\% \pm 2.55\%$

56.89%+2.90%

96.59% +0.45%

 $90.19\% \pm 0.71\%$

OP12PP1

PP12OP1

OPe2PPI

PP12OPe

CD2CO

CO2CD

41.47%

40.07%

41.47%

43.13%

14.59%

3.81%

		Average Accuracy		Max Accuracy		Min Accuracy	
	Task	RLG	CM	RLG	CM	RLG	CM
wo datasets)	G2A	72.70%±6.14%	44.89%±0.40%	83.50%	56.23%	57.50%	43.77%
,, o datasets)	A2G OPe2OPl	$57.21\% \pm 3.96\% \ 60.15\% \pm 3.16\%$	50.97%±5.21% 49.76%±5.79%	66.00 <i>%</i> 66.07 <i>%</i>	57.17% 59.93%	50.17% 52.40%	43.67% 40.07%
	OP12OPe	$58.08\% \pm 2.65\%$	$49.4\% \pm 5.01\%$	66.40%	56.87%	50.80%	43.13%

64.33%

68.00%

61.47%

61.47%

97.22%

91.56%

TABLE VI: The classification results for RLG and CM.

TABLE VII:	The cla	assification	results for	GLG a	nd CM

50.70%±5.24%

49.76%±5.79%

 $50.70\% \pm 5.24\%$

38.94%+45.17%

37.25%±33.37%

49.4% + 5.01%

		Average Accuracy		Max Accura		racy Min Accuracy	
Field	Task	GLG	CM	GLG	CM	GLG	CM
	G2A	78.18%±1.53%	44.89%±0.40%	81.33%	56.23%	75.67%	43.77%
Credit Assessment (Two datasets)	A2G	$61.25\% \pm 2.1\%$	$50.97\% \pm 5.21\%$	65.50%	57.17%	56.00%	43.67%
	OPe2OPl	$62.10\% \pm 1.63\%$	$49.76\% \pm 5.79\%$	64.47%	59.93%	59.07%	40.07%
	OPl2OPe	$59.54\% \pm 0.85\%$	$49.4\% \pm 5.01\%$	62.13%	56.87%	57.93%	43.13%
Tt Cl:6ti (O t-tt)	OP12PP1	$59.62\% \pm 1.54\%$	$50.70\% \pm 5.24\%$	62.07%	58.40%	57.67 %	41.47%
Text Classification (One dataset)	PP12OP1	$65.57\% \pm 0.79\%$	$49.76\% \pm 5.79\%$	66.67%	59.93%	65.00%	40.07%
	OPe2PPl	$58.31\% \pm 0.83\%$	$50.70\% \pm 5.24\%$	60.07%	58.40%	56.73%	41.47%
	PP12OPe	$58.81\% \pm 1.38\%$	$49.4\% \pm 5.01\%$	61.67%	56.87%	57.20%	43.13%
	CD2CO	$97.18\% \pm 0.15\%$	$38.94\% \pm 45.17\%$	97.22%	96.19%	96.93%	3.81%
Cancer Detection (Two datasets)	CO2CD	$90.22\% \pm 0.26\%$	$37.25\% \pm 33.37\%$	90.69%	85.41%	89.63%	14.59%

to reach in the text classification tasks than in the other two tasks. This result indicates that text classification tasks lose more information when transferring knowledge from the source domain to the target domain.

Field

Credit Assessment (Tw

Text Classification (One dataset)

Cancer Detection (Two datasets)

Figure 2 shows the results of each model across 50 experiments to better illustrate the classification effectiveness of the RLG and the GLG models. Clearly, RLG and GLG outperform the other models in terms of accuracy and stability.

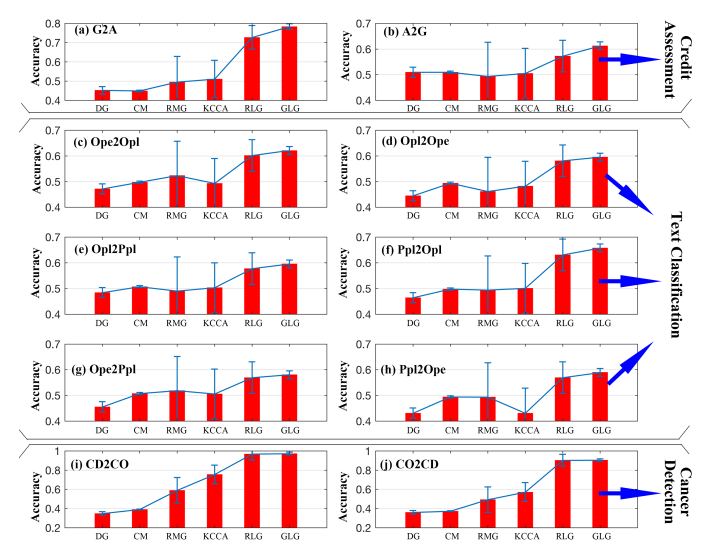


Fig. 2: The classification results of the proposed models and benchmarks.

VI. CONCLUSIONS AND FURTHER STUDIES

58.40%

59.93%

58.40%

56.87%

96.19%

85.41%

52.53%

53.07%

51.40%

48.53%

95.17%

88.58%

This paper fills several theoretical gaps in the field of heterogeneous unsupervised domain adaptation. On a foundational level, we present an unsupervised knowledge transfer theorem that outlines the sufficient conditions to guarantee that knowledge is transferred correctly from a source domain to a heterogeneous and unlabeled target domain. Additionally, we prove that the theorem is able to avoid negative transfer with at least one type of mapping function - LMM in this case. The theorem incorporates a distance metric, based on principal angles, to help construct homogeneous representations for heterogeneous domains. This metric shows the extent to which homogeneous representations have preserved the geometric distance between the original domains, and reveals the relationship between two heterogeneous feature spaces. The theorem, the distance metric, and the LMM mapping function are presented within the GLG model, which optimizes (minimizes) the principal angle-based metric to construct homogeneous representations for heterogeneous domains, then transfers knowledge across the homogeneous representations using a geodesic flow kernel. The overall efficacy of the GLG model was tested with five public datasets on three practical tasks: cancer detection, credit assessment, and text classification. The model demonstrated superior performance over the current benchmarks in all evaluation criteria.

Our future research will focus on three streams: 1) a multiple-domain HeUDA model; 2) a knowledge ensemble model to preserve knowledge of the unlabeled target domain; 3) an effective model to help improve the accuracy of prediction engines with some labeled instances in the target domain.

		Models						
Field	Task	A1	DR	CM	RMG	KCCA	RLG	GLG
Credit Assessment	G2A	50.00%	45.19%±1.96%	44.89%±0.40%	49.46%±13.31%	51.05%±9.72%	72.70%±6.14%	78.18%±1.53%
(Two datasets)	A2G	50.00%	$50.92\% \pm 1.06\%$	$50.97\% \pm 5.21\%$	$49.34\% \pm 5.2\%$	$50.52\% \pm 4.64\%$	$57.21\% \pm 3.96\%$	$61.25\% \pm 2.1\%$
(1wo datasets)	OPe2OP1	50.00%	$47.17\% \pm 3.14\%$	49.76%±5.79%	$52.36\% \pm 5.20\%$	$49.28\% \pm 3.22\%$	$60.15\% \pm 3.16\%$	$62.10\% \pm 1.63\%$
	OP12OPe	50.00%	$44.47\% \pm 1.60\%$	$49.4\% \pm 5.01\%$	$46.14\% \pm 5.10\%$	$48.19\% \pm 3.66\%$	$58.08\% \pm 2.65\%$	$59.54\% \pm 0.85\%$
Text Classification	OP12PP1	50.00%	$48.38\% \pm 5.51\%$	$50.70\% \pm 5.24\%$	$48.98\% \pm 5.84\%$	$50.27\% \pm 3.21\%$	$57.71\% \pm 2.50\%$	$59.62\% \pm 1.54\%$
(One dataset)	PP12OP1	50.00%	$46.37\% \pm 4.09\%$	49.76%±5.79%	$49.34\% \pm 5.58\%$	$50.03\% \pm 3.64\%$	$63.07\% \pm 3.11\%$	$65.57\% \pm 0.79\%$
,	OPe2PP1	50.00%	$45.52\% \pm 2.54\%$	$50.70\% \pm 5.24\%$	$51.83\% \pm 4.99\%$	$50.52\% \pm 3.52\%$	$56.88\% \pm 2.55\%$	$58.31\% \pm 0.83\%$
	PP12OPe	50.00%	$43.07\% \pm 1.75\%$	$49.4\% \pm 5.01\%$	$49.35\% \pm 4.88\%$	$43.07\% \pm 1.75\%$	$56.89\% \pm 2.90\%$	$58.81\% \pm 1.38\%$
Cancer Detection	CD2CO	65.01%	$34.62\% \pm 17.25\%$	$38.94\% \pm 45.17\%$	$58.92\% \pm 27.88\%$	$75.50\% \pm 15.19\%$	$96.59\% \pm 0.45\%$	$97.18\% \pm 0.15\%$
(Two datasets)	CO2CD	62.74%	$35.87\% \pm 7.56\%$	$37.25\% \pm 33.37\%$	$49.18\% \pm 20.87\%$	$57.10\% \pm 6.30\%$	$90.19\% \pm 0.71\%$	$90.22\% \pm 0.26\%$

TABLE VIII: The classification results for A1, DG, CM, RMG, KCCA, RLG, and GLG.

ACKNOWLEDGMENT

The work presented in this paper was supported by the Australian Research Council under Discovery Grant DP170101632.

REFERENCES

- S. J. Pan and Q. Yang, "A survey on transfer learning," *IEEE Transactions on Knowledge and Data Engineering*, vol. 22, no. 10, pp. 1345–1359, 2010.
- [2] J. Lu, V. Behbood, P. Hao, H. Zuo, S. Xue, and G. Zhang, "Transfer learning using computational intelligence: A survey," *Knowledge-Based Systems*, vol. 80, pp. 14–23, 2015.
- [3] L. Shao, F. Zhu, and X. Li, "Transfer learning for visual categorization: A survey," *IEEE Trans. Neural Netw. Learning Syst.*, vol. 26, no. 5, pp. 1019–1034, 2015.
- [4] B. Gong, K. Grauman, and F. Sha, "Learning kernels for unsupervised domain adaptation with applications to visual object recognition," *International Journal of Computer Vision*, vol. 109, no. 1-2, pp. 3–27, 2014
- [5] Y. Luo, T. Liu, Y. Wen, and D. Tao, "Online heterogeneous transfer metric learning," in *Proceedings of the 27th International Joint Conference on Artificial Intelligence*, Stockholm, Sweden, 2018, pp. 2525–2531.
- [6] Y. Yan, Q. Wu, M. Tan, M. K. Ng, H. Min, and I. W. Tsang, "Online heterogeneous transfer by hedge ensemble of offline and online decisions," *IEEE Trans. Neural Netw. Learning Syst.*, vol. 29, no. 7, pp. 3252–3263, 2018.
- [7] L. Yang, L. Jing, J. Yu, and M. K. Ng, "Learning transferred weights from co-occurrence data for heterogeneous transfer learning," *IEEE Trans. Neural Netw. Learning Syst.*, vol. 27, no. 11, pp. 2187–2200, 2016.
- [8] H. H. Zhuo and Q. Yang, "Action-model acquisition for planning via transfer learning," *Artificial Intelligence*, vol. 212, pp. 80–103, 2014.
- [9] R. A. C. Bianchi, L. A. Celiberto, P. E. Santos, J. P. Matsuura, and R. Lopez De Mantaras, "Transferring knowledge as heuristics in reinforcement learning: A case-based approach," *Artificial Intelligence*, vol. 226, pp. 102–121, 2015.
- [10] T. T. Nguyen, T. Silander, Z. Li, and T. Y. Leong, "Scalable transfer learning in heterogeneous, dynamic environments," *Artificial Intelli*gence, vol. 247, pp. 70–94, 2017.
- [11] E. Chalmers, E. B. Contreras, B. Robertson, A. Luczak, and A. J. Gruber, "Learning to predict consequences as a method of knowledge transfer in reinforcement learning," *IEEE Trans. Neural Netw. Learning Syst.*, vol. 29, no. 6, pp. 2259–2270, 2018.
- [12] L. Zhao, S. J. Pan, and Q. Yang, "A unified framework of active transfer learning for cross-system recommendation," *Artificial Intelligence*, vol. 245, pp. 38–55, 2017.
- [13] W. Pan and Q. Yang, "Transfer learning in heterogeneous collaborative filtering domains," Artificial Intelligence, vol. 197, pp. 39–55, 2013.
- [14] P. Zhao, S. C. H. Hoi, J. Wang, and B. Li, "Online transfer learning," Artificial Intelligence, vol. 216, pp. 76–102, 2014.
- [15] Z. Ma, Y. Yang, F. Nie, N. Sebe, S. Yan, and A. G. Hauptmann, "Harnessing lab knowledge for real-world action recognition," *International Journal of Computer Vision*, vol. 109, no. 1-2, pp. 60–73, 2014.
- [16] R. Gopalan, R. Li, and R. Chellappa, "Unsupervised adaptation across domain shifts by generating intermediate data representations," *IEEE Transactions on Pattern Analysis and Machine Intelligence*, vol. 36, no. 11, pp. 2288–2302, 2014.

- [17] M. Ghifary, D. Balduzzi, W. B. Kleijn, and M. Zhang, "Scatter component analysis: A unified framework for domain adaptation and domain generalization," *IEEE Transactions on Pattern Analysis and Machine Intelligence*, vol. 39, no. 7, pp. 1414–1430, 2017.
- [18] N. Courty, R. Flamary, D. Tuia, S. Member, and A. Rakotomamonjy, "Optimal transport for domain adaptation," *IEEE Transactions on Pattern Analysis and Machine Intelligence*, vol. 39, no. 9, pp. 1853 – 1865, 2017
- [19] B. Fernando, A. Habrard, M. Sebban, and T. Tuytelaars, "Unsupervised visual domain adaptation using subspace alignment," in *Proceedings of* the 14th IEEE International Conference on Computer Vision, Sydney, Australia, 2013, pp. 2960–2967.
- [20] B. Sun and K. Saenko, "Subspace distribution alignment for unsupervised domain adaptation," in *Proceedings of the 26th British Machine Vision Conference*, Swansea, UK, 2015, pp. 1–10.
- [21] M. Gong, K. Zhang, T. Liu, D. Tao, C. Glymour, and I. Systems, "Domain adaptation with conditional transferable components," in *Proceedings of the 33nd International Conference on Machine Learning*, New York City, USA, 2016, pp. 2839–2848.
- [22] M. Long, J. Wang, J. Sun, and P. S. Yu, "Domain invariant transfer kernel learning," *IEEE Transactions on Knowledge and Data Engineering*, vol. 27, no. 6, pp. 1519–1532, 2015.
- [23] M. Long, H. Zhu, J. Wang, and M. I. Jordan, "Unsupervised domain adaptation with residual transfer networks," in *Proceedings of the* 30th Annual Conference on Neural Information Processing Systems, Barcelona, Spain, 2016, pp. 136–144.
- [24] M. Long, J. Wang, Y. Cao, J. Sun, and P. S. Yu, "Deep learning of transferable representation for scalable domain adaptation," *IEEE Transactions on knowledge and data engineering*, vol. 28, no. 8, pp. 2027–2040, 2016.
- [25] Y. Cao, M. Long, and J. Wang, "Unsupervised Domain Adaptation with Distribution Matching Machines," in *Proceedings of the 32nd AAAI* conference on Artificial Intelligence, 2018, pp. 2795–2802.
- [26] M. Long, J. Wang, G. Ding, J. Sun, and P. S. Yu, "Transfer joint matching for unsupervised domain adaptation," in *Proceedings of the* 27th IEEE Conference on Computer Vision and Pattern Recognition, Columbus, OH, USA, 2014, pp. 1410–1417.
- [27] B. Sun, J. Feng, and K. Saenko, "Return of Frustratingly Easy Domain Adaptation," in *Proceedings of the 30th AAAI Conference on Artificial Intelligence*, Phoenix, USA, 2016, pp. 2058–2065.
- [28] S. J. Pan, I. W. Tsang, J. T. Kwok, and Q. Yang, "Domain adaptation via transfer component analysis," *IEEE Transactions on Neural Networks*, vol. 22, no. 2, pp. 199–210, 2011.
- [29] A. Gretton, K. M. Borgwardt, M. J. Rasch, B. Schölkopf, and A. J. Smola, "A kernel two-sample test," *Journal of Machine Learning Research*, vol. 13, pp. 723–773, 2012.
- [30] Y. Shi, L. Angeles, and F. Sha, "Information-theoretical learning of discriminative clusters for unsupervised domain adaptation," in *Proceedings of the 29th International Conference on Machine Learning*, Edinburgh, UK, 2012, pp. 1079–1086.
- [31] M. Long, J. Wang, G. Ding, J. Sun, and P. S. Yu, "Transfer feature learning with joint distribution adaptation," in *IEEE International Conference on Computer Vision*, Sydney, Australia, 2013, pp. 2200–2207.
- [32] J. Shen, Y. Qu, W. Zhang, and Y. Yu, "Wasserstein distance guided representation learning for domain adaptation," in *Proceedings of the Thirty-Second AAAI Conference on Artificial Intelligence*, New Orleans, Louisiana, USA, 2018, pp. 4058–4065.
- [33] J. W. Mingsheng Long, Yue Cao and M. I. Jordan, "Learning transferable features with deep adaptation networks," in *Proceedings of the 32nd*

- International Conference on Machine Learning, Lille, France, 2015, pp. 97–105.
- [34] M. Long, H. Zhu, J. Wang, and M. I. Jordan, "Deep transfer learning with joint adaptation networks," in *Proceedings of the 34th International Conference on Machine Learning*, Sydney, NSW, Australia, 2017, pp. 2208–2217.
- [35] X. Shi, Q. Liu, W. Fan, and P. S. Yu, "Transfer across completely different feature spaces via spectral embedding," *IEEE Transactions on Knowledge and Data Engineering*, vol. 25, no. 4, pp. 906–918, 2013.
- [36] C. Wang and S. Mahadevan, "Heterogeneous domain adaptation using manifold alignment," in *Proceedings of the 22nd International Joint Conference on Artificial Intelligence*, Barcelona, Spain, 2011, pp. 1541–1546
- [37] B. Kulis, K. Saenko, and T. Darrell, "What you saw is not what you get: Domain adaptation using asymmetric kernel transforms," in *Proceedings* of the 24th IEEE Computer Society Conference on Computer Vision and Pattern Recognition, Colorado Springs, USA, 2011, pp. 1785–1792.
- [38] W. Li, L. Duan, D. Xu, and I. W. Tsang, "Learning with augmented features for supervised and semi-supervised heterogeneous domain adaptation," *IEEE Transactions on Pattern Analysis and Machine Intelligence*, vol. 36, no. 6, pp. 1134–1148, 2014.
- [39] M. Xiao and Y. Guo, "Feature space independent semi-supervised domain adaptation via kernel matching," *IEEE Transactions on Pattern Analysis and Machine Intelligence*, vol. 37, no. 1, pp. 54–66, 2015.
- [40] H. V. Nguyen, H. T. Ho, S. Member, and V. M. Patel, "DASH-N: Joint hierarchical domain adaptation and feature learning," *IEEE Transactions* on *Image Processing*, vol. 24, no. 12, pp. 5479–5491, 2015.
- [41] Y. Yan, W. Li, M. K. P. Ng, M. Tan, H. Wu, H. Min, and Q. Wu, "Learning discriminative correlation subspace for heterogeneous domain adaptation," in *Proceedings of the 26th International Joint Conference* on Artificial Intelligence, Melbourne, Australia, 2017, pp. 3252–3258.
- [42] Y. Yan, W. Li, H. Wu, H. Min, M. Tan, and Q. Wu, "Semi-supervised optimal transport for heterogeneous domain adaptation," in *Proceedings* of the 27th International Joint Conference on Artificial Intelligence, Stockholm, Sweden, 2018, pp. 2969–2975.
- [43] J. T. Zhou, S. J. Pan, I. W. Tsang, and Y. Yan, "Hybrid Heterogeneous Transfer Learning through Deep Learning," in *Proceedings of the 28th AAAI Conference on Artificial Intelligence*, Québec City, Canada, 2014, pp. 2213–2219.
- [44] P. Wei, Y. Ke, and C. K. Goh, "A General Domain Specific Feature Transfer Framework for Hybrid Domain Adaptation," *IEEE Transactions* on Knowledge and Data Engineering, vol. Accepted, 2018.
- [45] Y. R. Yeh, C. H. Huang, and Y. C. F. Wang, "Heterogeneous domain adaptation and classification by exploiting the correlation subspace," *IEEE Transactions on Image Processing*, vol. 23, no. 5, pp. 2009–2018, 2014.
- [46] K. Ye and L.-H. Lim, "Schubert varieties and distances between subspaces of different dimensions," SIAM Journal on Matrix Analysis and Applications, vol. 37, no. 3, pp. 1176–1197, 2016.
- [47] Y. Wong, "Differential geometry of grassmann manifolds," Proceedings of the National Academy of Sciences, vol. 57, no. 3, pp. 589–594, 1967.
- [48] X.-S. Yang and S. Deb, "Engineering optimisation by cuckoo search," International Journal of Mathematical Modelling and Numerical Optimisation, vol. 1, no. 4, pp. 330–343, 2010.



Technology Sydney.

Feng Liu received the M.Sc. degree in probability and statistics and B.Sc. degree in pure mathematics from the School of mathematics and statistics, Lanzhou University, China, in 2015 and 2013, respectively. He is working toward the Ph.D. degree with the Faculty of En-gineering and Information Technology, University of Technology Sydney, Australia. His research interests include transfer learning and domain adaptation. He is a Member of the Decision Systems and e-Service Intelligence (DeSI) Research Laboratory, CAI, University of



Guangquan Zhang is an Associate Professor and Director of the Decision Systems and e-Service Intelligent (DeSI) Research Laboratory, Faculty of Engineer-ing and Information Technology, University of Technology Sydney, Australia. He received the Ph.D. degree in applied mathematics from Curtin University of Technology, Australia, in 2001. His research interests include fuzzy machine learning, fuzzy opti-mization, and machine learning and data analytics. He has authored four monographs, five textbooks, and 350 papers including 160 refer-eed

international journal papers.

Dr. Zhang has won seven Australian Research Council (ARC) Discov-ery Projects grants and many other research grants. He was awarded ARC QEII fellowship in 2005. He has served as a member of the editorial boards of several international journals, as a guest editor of eight special issues for IEEE transactions and other international journals, and co-chaired several international conferences and work-shops in the area of fuzzy decision-making and knowledge engineer-ing.



Jie Lu (F'18) is a Distinguished Professor and the Director of Centre for Artificial Intelligence at the University of Technology Sydney, Australia. She received the Ph.D. degree from Curtin University of Technology, Australia, in 2000.

Her main research expertise is in fuzzy transfer learning, decision support systems, concept drift, and recommender systems. She has published six research books and 400 papers in Artificial Intelligence, IEEE transactions on Fuzzy Systems and other refereed journals and conference proceedings.

She has won over 20 Australian Research Council (ARC) discovery grants and other research grants for over \$4 million. She serves as Editor-In-Chief for Knowledge-Based Systems (Elsevier) and Editor-In-Chief for International Journal on Computational Intelligence Systems (Atlantis), has delivered 20 keynote speeches at international conferences, and has chaired 10 international conferences. She is a Fellow of IEEE and Fellow of IFSA.